

## Structural Vibration Control for Broadband Noise Attenuation in Enclosures

**Kailash Krishnaswamy, Rajesh Rajamani**

*Department of Mechanical Engineering, University of Minnesota,  
Minneapolis, MN 55455, USA*

**Jong Jin Woo, Young Man Cho\***

*School of Mechanical and Aerospace Engineering,  
Seoul National University, Seoul 151-742, Korea*

This paper develops and evaluates several strategies for structural vibration control with the objective of attenuating broadband noise inside a rectangular enclosure. The strategies evaluated include model-independent collocated control, model-based feedback control and a new "modal-estimate" feedback strategy. Collocated control requires no knowledge of model parameters and enjoys the advantage of robustness. However, effective broadband noise attenuation with collocated control requires a large number of sensor-actuator pairs. Model-based controllers, on the other hand, can be theoretically effective even with the use of a single actuator. However, they suffer from a lack of robustness and are unsuitable from a practical point of view for broadband structural vibration applications where the dynamic models are of large order and poorly known. A new control strategy is developed based on attenuating a few structural vibration modes that have the best coupling with the enclosure acoustics. Broadband attenuation of these important modes can be achieved using a single actuator, a limited number of accelerometers and limited knowledge of a few modal functions. Simulation results are presented to demonstrate the effectiveness of the developed strategy.

**Key Words :** Structural Control, Noise Attenuation, Vibration Control, Acoustic Enclosure

### 1. Introduction

In recent years, much research effort has been directed towards both the prediction and control of cabin noise within commercial turbo-prop aircraft, helicopters, automobiles and elevators (MacMartin, 1994; Kuo and Morgan, 1999; Simpson et al., 1991; Fuller and Gibbs, 1994; Silcox et al., 1990). The broadband control of sound in such enclosures is a challenging problem

that has yet to be successfully addressed. In this paper we address this problem for the particular case of structure-borne noise (noise created by structural vibrations).

The concept of controlling structural vibrations to reduce transmitted or radiated noise is not new (Watreman, Kaptein and Sarin, 1983) and has been investigated by a variety of researchers (Simpson et al., 1991; Fuller et al., 1992; Silcox et al., 1992; Fuller and Gibbs, 1994; Silcox et al., 1990; Rossetti et al., 1994). However, most of the literature on this subject uses sound pressure feedback from within the enclosure. The approach in this paper, on the other hand, is to do purely structural control using feedback of structural vibration sensors, but with the objective of reducing noise transmission into the enclosure.

The paper is organized as follows. Section 2

---

\* Corresponding Author,

E-mail : ymcho85@snu.ac.kr

TEL : +82-2-880-1694; FAX : +82-2-883-1513

School of Mechanical and Aerospace Engineering,  
Seoul National University, Seoul 151-742, Korea.  
(Manuscript Received October 14, 2004; Revised May 31, 2005)

briefly describes an analytical simulation model for the structural acoustic vibrations in a paneled box and motivates the approach of structural vibration control as opposed to direct acoustic control. Section 3 evaluates the performance of LQR and collocated structural control algorithms in attenuating broadband enclosure noise. The ineffectiveness and disadvantages of both these controllers are discussed. Section 4 describes the coupling between the acoustic noise radiated into the enclosure and the individual structural modes of the vibrating panel. We show that a few of the modes couple very well with the acoustics and are responsible for a major fraction of the acoustic energy radiated into the enclosure. Section 5 then describes the design of a new control algorithm based on controlling important individual modes of vibration. The design of an estimator to estimate modal signals from accelerometer measurements is also presented. Section 6 evaluates the performance of the estimator-based controller. Simulations are used to demonstrate both the attenuation of the important structural vibration modes as well as attenuation of acoustic pressure inside the enclosure.

## 2. System Description and Dynamic Modeling

In this paper a generic rectangular enclosure formed by a paneled box is considered. There are six panels: four on the sides and one each on the roof and floor of the box. It is assumed that noise is radiated into the enclosure from the vibrations of the flexible roof. Figure 1 shows a schematic of the structure. The frame of the structure is assumed to be made up of very stiff beam sections bolted to each other. The panels are  $1.59 \times 10^{-3}$  m thick aluminum sheets which are bolted onto the frames at the boundaries. The dimensions of the box are  $0.635 \times 0.889 \times 0.889$  meters. Many practical applications may have more than one panel on each side of the frame.

The enclosed acoustic cavity is a rectangular box for which closed form representations of the modes exist (Blevins, 1979). Similarly, the panels are rectangular and are assumed to have simply

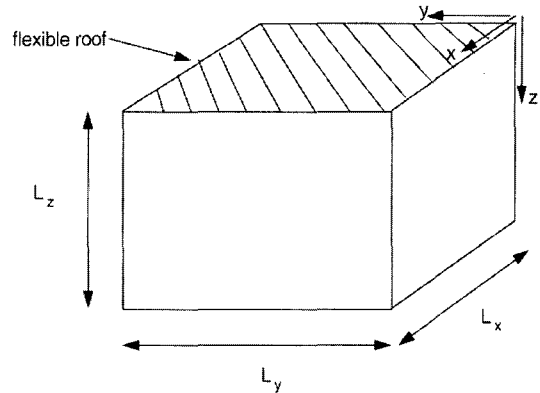


Fig. 1 Schematic of paneled box

supported boundary conditions. This is a reasonable assumption for a panel bolted onto the frame. Closed form representations for the normal modes exist (Blevins, 1979) for a thin rectangular plate with simply supported boundary conditions.

The wave numbers  $\lambda_{ij}$  and the structural resonance frequencies for the plate  $f_{ij}$  are given by (Blevins, 1979):

$$\lambda_{ij}^2 = \pi^2 \left[ i^2 + j^2 \left( \frac{a^2}{b^2} \right) \right] \quad (1)$$

$$f_{ij}^2 = \frac{\lambda_{ij}^2}{2\pi a^2} \left[ \frac{Eh^3}{12\gamma(1-\nu^2)} \right]^{\frac{1}{2}} \text{ (Hz)}$$

where  $i, j = 1, 2, 3, \dots, 8$  are the indices in the  $x$  and  $y$  coordinates of the local coordinate system attached to the plate.  $a, b$  are the length of the sides of the plate,  $h$  is the thickness,  $\gamma$  is the mass per unit area,  $E$  is the Young's modulus and  $\nu$  is the Poisson's ratio. The corresponding modal functions of the plate are mutually orthogonal and are given by

$$\psi_m(x, y) = \psi_{ij}(x, y) = \sin\left(\frac{i\pi x}{a}\right) \sin\left(\frac{j\pi y}{b}\right) \quad (2)$$

Similarly, for the acoustic cavity, the natural frequencies are given by [3]:

$$f_{rst} = \frac{c}{2} \left[ \frac{r^2}{L_x^2} + \frac{s^2}{L_y^2} + \frac{t^2}{L_z^2} \right]^{\frac{1}{2}} \quad (3)$$

where  $c$  is the speed of sound in air,  $L_x, L_y$  and  $L_z$  are the length of the sides of the box and  $r, s, t$  are the indices in the three coordinate directions

of the box. The corresponding acoustic modal functions are given by

$$F_n(x, y, z) = F_{rst}(x, y, z) = \cos\left(\frac{r\pi x}{L_x}\right) \cos\left(\frac{s\pi y}{L_y}\right) \cos\left(\frac{t\pi z}{L_z}\right) \quad (4)$$

A total of 64 structural modes and 10 acoustic modes are used in the model. The total number of acoustic modes have been chosen so as to span the broadband frequency range 0–500 Hz. The order of the coupled system is therefore 74 and the state-space model is of size 148.

The size of the state-space model for the 0–500 Hz broadband problem gives us an indication of how tough the broadband acoustic control problem is. An adaptive controller based on active noise cancellation would be complicated to design and implement because of the large number (10) of acoustic degrees of freedom to be controlled. Though the number of structural degrees of freedom is also high for this particular broadband range, the number of structural modes increase linearly with frequency while the number of acoustic modes increase cubically, as shown in Fig. 2. For active control of sound in the 0–1000 Hz range, one might consider controlling the structural modes directly or controlling a few important structural modes instead of doing acoustic control. This motivation will become clearer later in the paper.

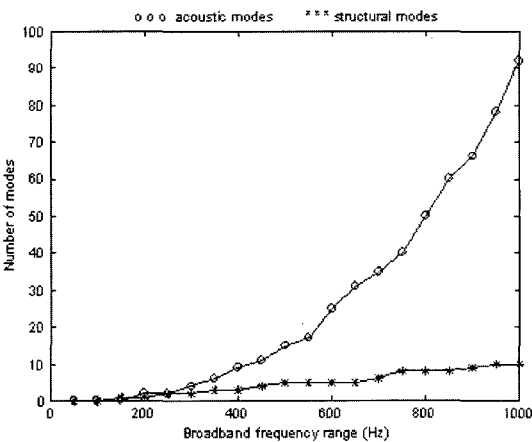


Fig. 2 Number of structural and acoustic modes as a function of frequency range

## 2.1 Acoustic dynamics in the enclosure

Using the modal approach to modeling (Srinivasan and Rajamani, 1998), the acoustic pressure  $p(x, y, z, t)$  at any point in the enclosure can be expressed as a series in terms of the natural acoustic modes of the enclosure:

$$p(x, y, z, t) = -\rho_o \dot{\varphi} \quad (5)$$

$$\varphi(x, y, z, t) = \sum_n a_n(t) F_n(x, y, z)$$

where  $F_n(x, y, z)$  is the  $n$ -th acoustic mode shape,  $a_n(t)$  are the weights that are functions of time,  $\rho_o$  is the nominal density of air, and  $\varphi(x, y, z, t)$  is the acoustic mode.

The dynamic equation for each acoustic mode is given by [3]:

$$N_n V [\ddot{a}_n + 2\xi_a \omega_n \dot{a}_n + \omega_n^2 a_n] = A_F c_o^2 \sum_m L_{nm} \dot{q}_m \quad (6)$$

where  $N_n$  is the generalized modal mass,  $V$  is the volume of the enclosure,  $\omega_n = 2\pi f_{rst}$ ,  $\xi_a$  is the acoustic modal damping ratio,  $A_F$  is the area of the vibrating roof,  $c_o$  is the speed of sound in air,  $q_m(t)$  is the contribution (weight) of the  $m$ -th structural mode shape and  $L_{nm}$  is the vibro-acoustic coupling term defined by

$$L_{nm} = \frac{1}{A_F} \int_{A_F} \psi_m F_n dA \quad (7)$$

## 2.2 Structural dynamics of the panels

The structural vibrations of the panel can be similarly expressed as a series in terms of the structural modal functions as

$$w(x, y, t) = \sum_m q_m(t) \psi_m(x, y) \quad (8)$$

It is to be noted that in the case where a thin flexible membrane is involved, it might be important to consider the influence of the acoustic pressure on the structural vibrations. Since this paper consider a 1.59 mm thick aluminum panel, it is very reasonable to ignore the influence of the acoustic pressure on the structural vibrations. Ignoring the effect of acoustic pressure variations on the structural vibrations of the panel (a reasonable assumption), the dynamic equation for each structural mode is given by

$$M_m [\ddot{q}_m + \omega_m^2 q_m] = Q_m^E \quad (9)$$

where  $M_m$  is the structural modal mass,  $\omega_m = 2\pi f_{ij}$  and  $Q_m^E$  is the generalized force due to external agents acting on the panel given by

$$Q_m^E = - \int_{A_p} p^E(x, y) \psi_m(x, y) dA \quad (10)$$

We will assume that the external forces on the panel include a point force actuator at the center of the panel and a disturbance force that varies with time but acts uniformly over the panel. For a point force actuator,  $p^E(x, y)$  is a Dirac-delta function at the location of the actuator. For a uniform pressure force acting on the panel,  $p^E(x, y)$  is a constant.

For multiple modes in the panels and acoustics, the coupled matrix equations of motion in 2nd order form in the presence of damping are given by (Srinivasan and Rajamani, 1998):

$$\begin{aligned} & \begin{bmatrix} M^S & 0 \\ 0 & M^A \end{bmatrix} \begin{Bmatrix} \ddot{q} \\ \ddot{a} \end{Bmatrix} + \begin{bmatrix} C^S & 0 \\ 0 & C^A \end{bmatrix} \begin{Bmatrix} \dot{q} \\ \dot{a} \end{Bmatrix} \\ & + \begin{bmatrix} 0 & 0 \\ G_2 & 0 \end{bmatrix} \begin{Bmatrix} \dot{q} \\ \dot{a} \end{Bmatrix} + \begin{bmatrix} K^S & 0 \\ 0 & K^A \end{bmatrix} \begin{Bmatrix} q \\ a \end{Bmatrix} = \begin{bmatrix} D \\ 0 \end{bmatrix} u \quad (11) \\ & y = H_1 \begin{Bmatrix} q \\ a \end{Bmatrix} + H_2 \begin{Bmatrix} \dot{q} \\ \dot{a} \end{Bmatrix} + H_3 u \end{aligned}$$

where  $M^S$ ,  $M^A$  are the mass matrices for the panels and the acoustic cavity,  $C^S$ ,  $C^A$  and  $K^S$ ,  $K^A$  are the damping and the stiffness matrices respectively.  $G_2$  is the vibro-acoustic coupling term and  $D$  is the input matrix which determines where the actuator and disturbance input forces act on the panel.  $H_1$ ,  $H_2$  and  $H_3$  are the output matrices which determine the variables available for measurement. In this paper, the output signals are assumed to be accelerometers at various locations on the panel.

### 3. Evaluation of LQR and Collocated Structural Control Laws for Structural Attenuation

Two well-known structural vibration control strategies are evaluated in this section and their performance in terms of enclosure noise attenuation studied. The parameters used in the simula-

tion for the excited plate are  $a=0.889$  m,  $b=0.635$  m,  $h=0.0016$  m,  $E=72 \times 10^9$  N/m<sup>2</sup>,  $\nu=0.32$  and  $\gamma=2800 \times 0.016$  kg/m<sup>2</sup> corresponding to a density of 2800 kg/m<sup>3</sup> for aluminum. The parameters used for the acoustic enclosure are  $L_x=a$ ,  $L_y=b$  and  $L_z=a$ . The damping ratio was assumed to be 1% for all the structural and acoustic modes.

#### 3.1 The optimal linear quadratic regulator (LQR)

Using a single force actuator at the center of the panel, the LQR controller can be used to control the vibrations of the panel. Full-state feedback (knowledge of all the modal displacements  $q_m(t)$  and their derivatives  $\dot{q}_m(t)$ ) is assumed. Figure 3 shows the disturbance to acceleration transfer function at the center of the panel. The state weighting matrix  $Q$  is assumed to be identity while the control weighting matrix  $R$  is assumed to be 0.001. We see that the LQR controller damps the resonant peaks of the acceleration transfer function and provides good vibration attenuation at the resonant frequencies.

Figure 4 shows the disturbance force to acoustic noise transfer function, with the microphone assumed to be at one of the 4 corners of the enclosure closest to the vibrating panel. We see that while the acoustic noise is reduced at the resonant frequency of 100 Hz, noise attenuation

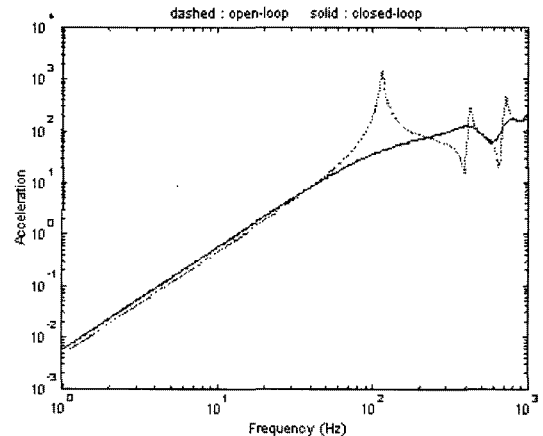


Fig. 3 Disturbance to acceleration transfer function at the center of the panel

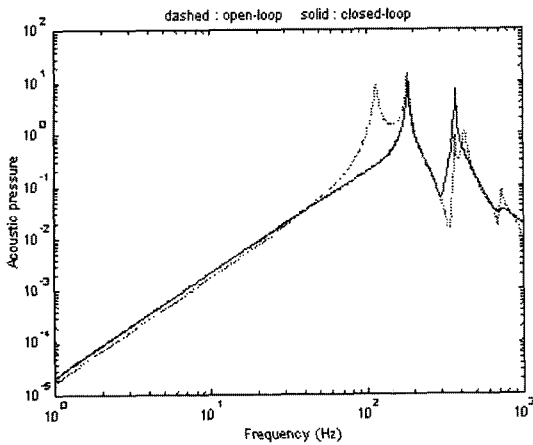


Fig. 4 Disturbance to acoustic noise transfer function with LQR controller (with microphone at near corner of enclosure)

is not obtained at frequencies beyond 100 Hz. This indicates that reducing the resonant vibrations of the panel is not sufficient to yield broadband enclosure noise attenuation.

The LQR controller with simple-minded  $Q$  and  $R$  weights described above thus fails to meet the performance specification of broadband noise attenuation. In addition, the LQR controller is unrealistic because it requires feedback of all states which could only be obtained by using a huge grid of position and velocity sensors.

### 3.2 Collocated control

Collocated control is often used in vibration attenuation applications [2]. The panel is assumed to have a grid of collocated point force actuators and accelerometers. The mass effect of the point force actuators and accelerometers are neglected in this analytic study. The velocity at each location is obtained by integrating the accelerometer and then fed back to the actuator at the same location with an appropriate gain :

$$u_i = -k_i \dot{z}_i$$

where  $\dot{z}_i$  is the absolute velocity at the location of the  $i$ -th accelerometer. The transfer function from collocated velocity to force is dissipative and this guarantees stability of the closed-loop system [2]. This control technique is robust and practical, requiring absolutely no knowledge of plant

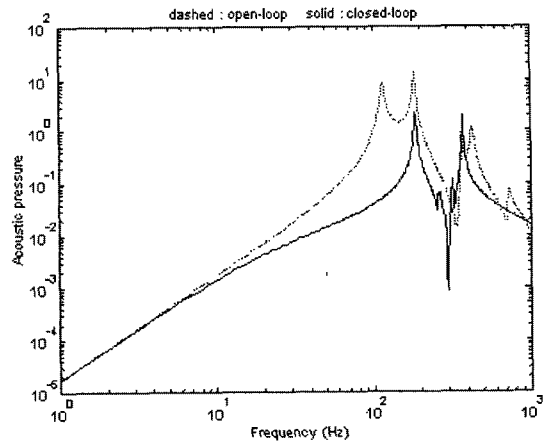


Fig. 5 Disturbance to acoustic noise transfer function with collocated control (with microphone at near corner of enclosure)

parameters. The disadvantage of the technique lies in the fact that it requires many sensors and actuators in order to be effective and is therefore expensive. Figure 5 shows the acoustic noise attenuation performance of the collocated controller with a grid of 36 sensor-actuator pairs. While the performance is superior to that of the LQR controller and significant noise attenuation is obtained up to a frequency of 200 Hz, we see that the expense of 36 sensor-actuator pairs cannot be adequately justified. The performance specification of broadband attenuation up to 500 Hz is not met.

## 4. Study of Structural-Acoustic Coupling

This section looks at the coupling between structural and acoustic vibrations, with the objective of identifying the structural modes that couple strongly with acoustic radiation.

From Eq.(6), the relation between the structural and acoustic contribution factors is seen to be given by

$$\frac{a_n}{q_m} = G_{1n}(s) L_{nm} \tag{12}$$

where  $G_{1n}(s) = \frac{c_0^2 A_F}{VN_n(s^2 + 2\xi_a \omega_n s + \omega_n^2)}$  for each value of  $n$  and  $m$ .

The total acoustic energy contributed by each structural mode to all the acoustic modes can be calculated as a sum of kinetic and potential energies :

$$E_a = \frac{1}{2} N_n V \dot{a}_n^2 + \frac{1}{2} N_n V \omega_n^2 a_n^2 \quad (13)$$

or

$$\frac{E_a}{q_m^2} = \left[ \sum_n \frac{1}{2} N_n V |j\omega G(j\omega)|^2 L_{nm}^2 + \frac{1}{2} N_n V \omega_n^2 |G(j\omega)|^2 L_{nm}^2 \right] \quad (14)$$

The acoustic energy contribution of each structural mode has been calculated by integrating the right-hand-side of Eq. (14) over the broadband frequency range of interest (0-300 Hz). The result is shown in Fig. 6 in terms of the fraction of total acoustic energy contributed by each of the structural modes.

It can be concluded from the figure that the first structural mode (with indices (1, 1)) couples most with the acoustics and radiates the most acoustic energy. Also the first few structural modes are the strongest acoustic radiators. It is therefore expected that suppression of the first few structural modes will yield significant levels of sound attenuation in the enclosure. In particular, suppression of the first structural mode ( $q_1$ ) will be sufficient to yield significant noise reduction.

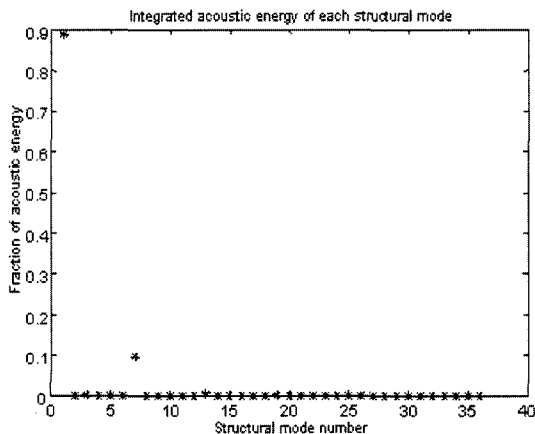


Fig. 6 Fraction of acoustic energy contributed by each structural mode

### 5. New Modal-Feedback Control Strategy

The inability of the LQR controller to provide broadband noise attenuation can be understood in light of the results of section 4. Figure 7 shows the magnitude of the transfer function from disturbance to  $\ddot{q}_1$  using the LQR controller. We see that while the resonant peak of this mode is well attenuated by the LQR controller, the magnitude of  $\ddot{q}_1$  is not attenuated at frequencies beyond the resonant frequency. Since the  $q_1$  mode is responsible for a significant fraction of the acoustic noise propagation into the enclosure, the LQR controller only manages to attenuate noise at the  $q_1$  resonant frequency but does not achieve broadband noise attenuation.

A new control technique is therefore sought so as to achieve broad band attenuation of the  $q_1$  mode. Additionally, a desirable characteristic of the new control law would be the requirement for less sensors compared to the LQR controller and less actuators compared to the collocated controller.

The following control law is proposed using a single actuator at the center of the panel

$$U = -k_a \dot{q}_1 - k_v q_1 \quad (15)$$

**Claim 1:** With the gains  $k_a$  and  $k_v$  appropriately chosen, the control law Eq. (15)

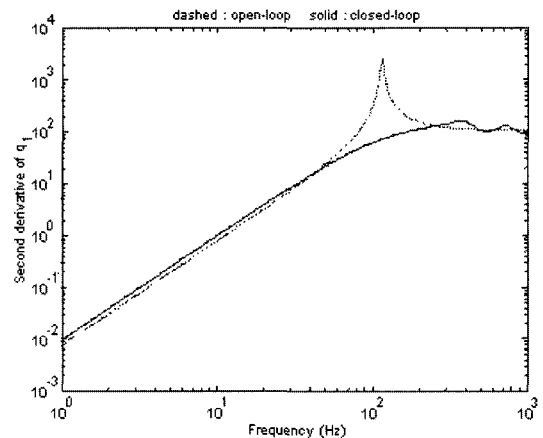


Fig. 7 Disturbance to  $\ddot{q}_1$  transfer function using the LQR controller

(a) provides broadband attenuation of the  $q_1$  mode and

(b) ensures that the magnitudes of all the modes  $q_2, q_3, \dots, q_m$  are bounded in the presence of a bounded disturbance force on the vibrating panel.

The proof of this claim is presented in the Appendix.

Having determined a control law suitable for broad band active noise attenuation, it is now necessary to design a suitable estimator for an estimate of the  $\ddot{q}_1$  mode in order to enable implementation of the control law. For this purpose, a grid of  $n_{acc}$  accelerometers, at locations  $(x_i, y_i)$  are used. The output,  $a(x_i, y_i)$  measured at a location  $(x_i, y_i)$  by the corresponding accelerometer is given by

$$a(x_i, y_j) = \sum_{m=1}^{\infty} \psi_m(x_i, y_j) \ddot{q}_m \quad (16)$$

if an infinite number of structural modes for the panel is assumed. For a given frequency range of significance, assume the number of significant structural modes is  $e$ . The vector of accelerations  $a(x_i, y_i)$  can then be approximated as

$$A = \begin{bmatrix} a(x_1, y_1) \\ a(x_2, y_2) \\ \vdots \\ a(x_{n_{acc}}, y_{n_{acc}}) \end{bmatrix} = \Psi \begin{bmatrix} \ddot{q}_1 \\ \ddot{q}_2 \\ \vdots \\ \ddot{q}_e \end{bmatrix} \quad (17)$$

where

$$\Psi = \begin{bmatrix} \psi_1(x_1, y_1) & \psi_k(x_1, y_1) & \dots & \psi_e(x_1, y_1) \\ \psi_1(x_2, y_2) & \psi_k(x_2, y_2) & \dots & \psi_e(x_2, y_2) \\ \vdots & \vdots & \ddots & \vdots \\ \psi_1(x_{n_{acc}}, y_{n_{acc}}) & \psi_k(x_{n_{acc}}, y_{n_{acc}}) & \dots & \psi_e(x_{n_{acc}}, y_{n_{acc}}) \end{bmatrix} \quad (18)$$

with the columns of the matrix  $\psi$  being the structural modes that are significant in the frequency range of interest calculated at the locations of the accelerometers. The number of accelerometers can be chosen to be equal to the number of significant modes so as to obtain an invertible square  $\psi$  matrix. The ‘modal acceleration’ state vector can then be estimated as

$$\begin{bmatrix} \hat{\ddot{q}}_1 \\ \vdots \\ \hat{\ddot{q}}_e \end{bmatrix} = \Psi^{-1} A \quad (19)$$

Note that once the broadband frequency region of interest has been defined, the modes of significance are then automatically defined. No matter how many modes of vibration the panel may have, the higher modes will not contribute in the broadband frequency of interest. Therefore the number of significant modes is fixed and independent of the total number of modes used in the panel model.

### 6. Results

From the estimated vector in Eq.(19), only the first mode is used for feedback. For the particular panel under consideration, 9 panel modes are found to be significant in the 0–500 Hz range. Of these, only the 4 symmetric modes are excited when the disturbance on the vibrating panel is uniform pressure. A grid of 4 accelerometers is therefore used to estimate the  $\ddot{q}_1$  mode. Figure 8 illustrates the results of the  $\ddot{q}_1$  estimation algorithm. Although the number of structural modes modeled in this simulation is 64, the use of 4 accelerometers is sufficient to accurately estimate  $\ddot{q}_1$  at all frequencies up to 1000 Hz. Figure 9 illustrates the result of  $\ddot{q}_1$  feedback. We observe significant attenuation of  $\ddot{q}_1$  (by a factor of 100) in the broadband 0–500 Hz range and attenuation by a factor of 1000 at the resonant frequency.

The effect of the attenuation of the  $q_1$  mode on

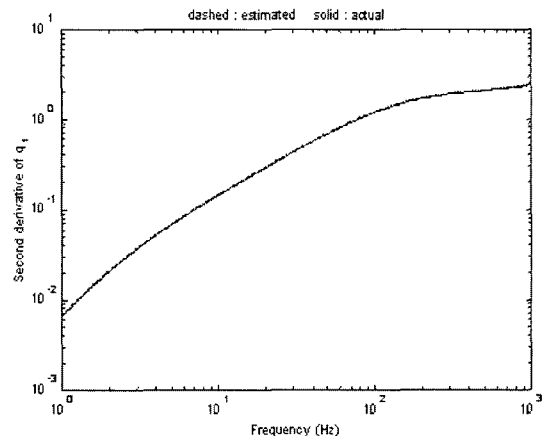
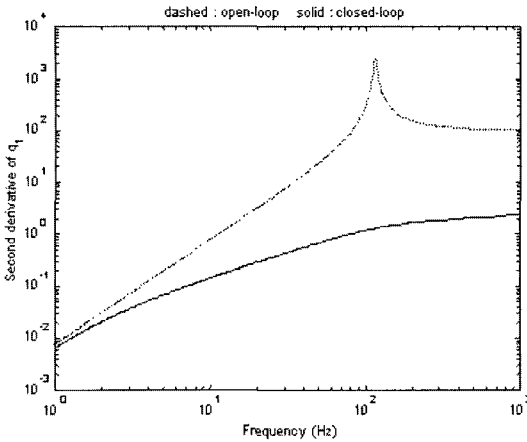
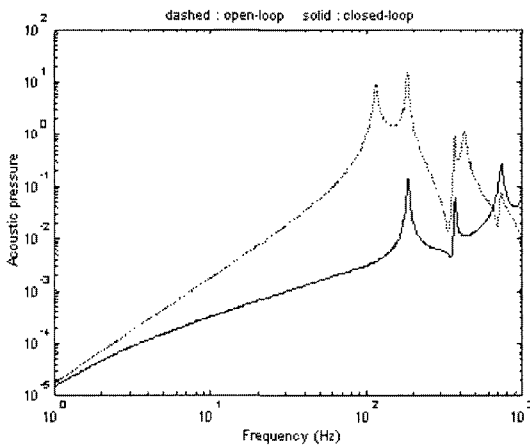


Fig. 8 Disturbance to  $\ddot{q}_1$  transfer function : estimated and actual



**Fig. 9** Disturbance to  $\ddot{q}_1$  transfer function: open-loop and closed-loop



**Fig. 10** Open-loop and closed-loop acoustic pressure at a near corner of the paneled box

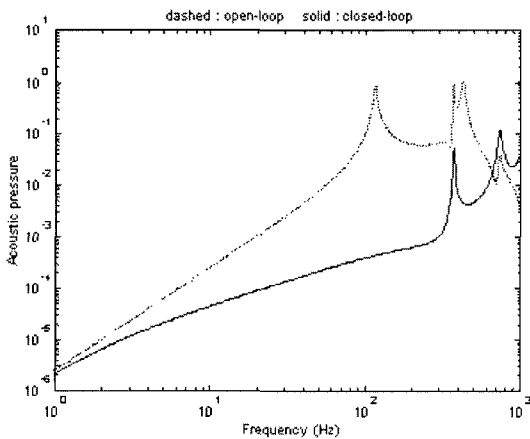


**Fig. 11** Open-loop and closed-loop acoustic pressure at the center of the paneled box

the enclosure acoustics is shown in Figs. 10 and 11. We observe significant broadband reduction in acoustic pressure (by more than a factor of 10 over the entire 0–500 Hz range).

## 7. Conclusions

Model-based and co-located controllers were evaluated for structural vibration control and their effect on noise attenuation in the enclosure studied. It was observed that neither controller was able to achieve broad band noise attenuation. They also have associated disadvantages. A new control strategy was developed based on identification and attenuation of the few structural vibration modes that have the best coupling with the enclosure acoustics. Broadband attenuation of these important modes was achieved using a single actuator, a limited number of accelerometers and limited knowledge of a few modal functions. Simulation results were presented to demonstrate the effectiveness of the developed strategy. The developed strategy is robust, uses limited knowledge of the plant, and achieves excellent attenuation with a single actuator and a grid of limited sensors.

## Acknowledgments

This research was supported by a grant from the Micro Thermal System Research Center through the Korea Science and Engineering Foundation.

## References

- Blevins, R. D., 1979, "Formulas for Frequency and Mode Shapes," Robert Krieger, Malabar, FL.
- Fuller, C. R. and Gibbs, G. P., 1994, "Active Control of Interior Noise in a Business Jet Using Piezo ceramic Actuators," Noise-Con 94.
- Fuller, C. R., Snyder, S. D., Hansen, C. H. and Silcox, R. J., 1992, "Active Control of Interior Noise in Model Aircraft Fuselages using Piezo ceramic Actuators," *AIAA Journal*, Vol. 30, pp. 2613~2617.
- Ha, H. T. R., 1995, "Vibration Control of



Rotor," *KSME International Journal*, Vol. 35, No. 10, pp. 917~923, 1225~5955.

Kuo, S. M. and Morgan, D. M., 1999, "Active Noise Control : A Tutorial Review," *Proceedings of the IEEE*, Vol. 87, No. 6.

MacMartin, D. G., 1996, "Colocated Structural Control for Reduction of Aircraft Cabin Noise," *Journal of Sound & Vibration*, Vol. 190, No. 1, pp. 105~119.

Oh, J. Y., 1993, "The Active Noise Control in Harmonic Enclosed Sound Fields (I) : Computer Simulation," *KSME International Journal*, Vol. 17, No. 5, pp. 1054~1065, 1225~5963, May.

Rossetti, D. J., Norris, M. A., Southward, S. C. and Sun, J. Q., 1994, "A Comparison of Speakers and Structural Based Actuators for Aircraft Cabin Noise Control," *Recent Advances in Active Control of Sound and Vibration*, VPI & SU, Technomic, Blacksburg, Virginia.

Silcox, R. J., Fuller, C. R. and Lester, H. C., 1990, "Mechanisms of Active Control in Cylindrical Fuselage Structures," *AIAA Journal*, Vol. 28, pp. 1397~1404.

Silcox, R. J., Lefebvre, S., Metcalf, V. L., Beyer, T. B. and Fuller, C. R., 1992, "Evaluation of Piezo ceramic Actuators for Control of Aircraft Interior Noise," *Proceedings of the DGLR/AIAA 14<sup>th</sup> Aeroacoustics Conference*, AIAA Paper No. 92-02-091, pp. 542~551.

Simpson, M. A., Luong, T. A., Fuller, C. R. and Jones, J. D., 1991, "Full Scale Demonstration Tests of Cabin Noise Reduction Using Active Vibration Control," *AIAA Journal of Aircraft*, Vol. 28, pp. 208~215.

Srinivasan, S. and Rajamani, R., 1998, "Acoustic Modeling of the Structural Acoustic Vibrations in a Paneled Box," *Mathematical Modeling of Systems*, Vol. 4, No. 2, pp. 148~161.

Waterman, E. H., Kaptein, D. and Sarin, S. L., 1983, "Fokker's Activities in Cabin Noise Control for Propeller Aircraft," *SAE Paper 830736*.

Soo Jeon, Hyeong-Joon Ahn and Dong-Chul Han, 2002, "Model Validation and Controller Design for Vibration Suppression of Flexible Rotor Using AMB," *KSME International Journal*, Vol. 16, No. 12, pp. 1583~1593.

Jae Kyung Shim and Sungsoo Na, 2003, "Mo-

deling and Vibration Feedback Control of Rotating Tapered Composite Thin-Walled Blade," *KSME International Journal*, Vol. 17, No. 3, pp. 380~390.

Chul hue Park and Hyun Chul Park, 2003, "Multiple-Mode Structural Vibration Control Using Negative Capacitive Shunt Damping," *KSME International Journal*, Vol. 17, No. 11, pp. 1650~1658.

Weui bong Jeong, Wan Suk Yoo, Woo Jin Jung, 2003, "Vibration and Noise Control of Structural Systems Using Squeeze Mode ER Mounts," *KSME International Journal*, Vol. 17, No. 12, pp. 1949~1960.

Kim, S. H. and Lee, J. M., 1998, "A Practical Method for Noise Reduction in a Vehicle Passenger Compartment," *ASME Journal of Vibration and Acoustics*, Vol.120(1), pp. 199~205.

Chul Ki Song, Jin Kwon Hwang, Jang Moo Lee, J. Karl Hedrick, 2003, "Active Vibration Control for Structural-Acoustic Coupling System of a 3-D Vehicle Cabin Model," *Journal of Sound and Vibration*, Vol. 267, pp. 851~865.

Dowell E. H. et al., 1977, "Acoustoelasticity : General Theory, Acoustic Natural Modes and Forced Response to Sinusoidal Excitation, including comparisons with Experiments," *Journal of Sound and Vibration*, Vol. 53(4), pp. 519~542.

## Appendix : Proof of Claim 1

The dynamic equation for the  $m^{\text{th}}$  mode of structural vibration can be expressed as

$$\frac{d^2 q_m}{dt^2} + 2\xi\omega_m \frac{dq_m}{dt} + \omega_m^2 q_m = a_{m1}U + a_{m2}D \quad (20)$$

where  $a_{m1}$  and  $a_{m2}$  are constant coefficients (refer Eq.(9) and [3]) and  $U$ ,  $D$  are the control input and the external disturbance acting on the system. The open loop transfer function from the disturbance to the  $q_1$  mode is then seen to be given by

$$G_{open-loop} = \frac{q_1}{D} = \frac{a_{12}}{s^2 + 2\xi\omega_1 s + \omega_1^2} \quad (21)$$

with  $s$  being the Laplace variable.

The feedback law  $U = -k_a \dot{q}_1 - k_v \dot{q}_1$  yields the

following closed loop disturbance to  $q_1$  mode transfer function

$$G_{closed-loop} = \frac{q_1}{D} = \frac{a_{12}}{(1+k_a)s^2 + (k_v + 2\xi\omega_1)s + \omega_1^2} \quad (22)$$

A suitable choice of  $k_v$  and  $k_a$  then provides the desired broadband attenuation of the  $q_1$  mode. The gain  $k_v$  attenuates the resonant peak of the  $q_1$  mode while the gain  $k_a$  attenuates the magnitude of the  $q_1$  mode at frequencies beyond the resonant frequency. Note that the high frequency asymptote of the transfer function in Eq.(22) is influenced purely by the gain  $k_a$ .  $\ddot{q}_1$  feedback is therefore necessary in order to obtain broadband

attenuation of  $q_1$ .

The influence of the control law on the other structural modes of the vibrating panel can be studied from the equation

$$\begin{aligned} \frac{d^2 q_m}{dt^2} + 2\xi\omega_m \dot{q}_m + \omega_m^2 q_m \\ = a_{m1}(-k_a \ddot{q}_1 - k_v \dot{q}_1) + a_{m2} D \end{aligned} \quad (23)$$

Since the unforced equation  $\frac{d^2 q_m}{dt^2} + 2\xi\omega_m \dot{q}_m + \omega_m^2 q_m = 0$  is asymptotically stable and the inputs  $\dot{q}_1$ ,  $\ddot{q}_1$  and  $D$  to Eq.(23) are all bounded, the states  $q_m$  and  $\dot{q}_m$  are guaranteed to be bounded for all the modes. This completes the proof.